MOLECULAR CORRELATE OF MOUSE EXECUTIVE FUNCTION. TOP-DOWN and BOTTOM-UP INFORMATION FLOWS COMPLEMENTATION by *Ntng* GENE PARALOGS

Pavel Prosselkov[1,2]*, Qi Zhang[1], Goto Hiromichi[1], Denis Polygalov[3], Thomas J. McHugh[3] and Shigeyoshi Itohara[1]*

[1]Laboratory for Behavioral Genetics, and [3]Laboratory for Circuit and Behavior Physiology, RIKEN Brain Science Institute, 351-0198 Saitama, Japan

[2]Department of Physiology, Faculty of Medicine, Saitama Medical University, Saitama 350-0495, Japan

*corresponding authors:

prosselkov@brain.riken.jp

sitohara@brain.riken.jp

Keywords: executive function, attention and impulsivity, working memory, learning, gene duplication, cognitive complement

ABSTRACT

Executive function (EF) is a regulatory construct of learning and a main characteristic of general cognitive abilities. Genetic variations underlying the architecture of cognitive phenotypes are likely to affect EF. Mice lacking one of *Ntng* gene paralogs, encoding the vertebrate brain-specific presynaptic Netrin-G proteins, exhibit prominent deficits in the EF control. Brain areas responsible for gating the bottom-up and top-down information flows differentially express *Ntng1* and *Ntng2,* distinguishing neuronal circuits involved in perception and cognition. As a result, high and low cognitive demand tasks (HCD and LCD, respectively) modulate *Ntng1* and *Ntng2* associations either with attention and impulsivity (AI) or working memory (WM), in a complementary manner. During the LCD *Ntng2*-supported neuronal gating of AI and WM dominates over the *Ntng1*-associated circuits. This is reversed during the HCD, when the EF requires a larger contribution of cognitive control, supported by *Ntng1*, over the *Ntng2* pathways. Since human *NTNG* orthologs have been reported to affect human IQ (1), and an array of neurological disorders (2), we believe that mouse *Ntng* gene paralogs serve an analogous role but influencing brain executive function.

INTRODUCTION

Executive function (EF) is a heterogeneous construct that can be viewed as a set of processes executively supervising cognitive behaviors (3). EF is an umbrella term for working memory (WM), attention and impulsivity (AI), and response inhibition, and is thought to account for the variance in cognitive performance (4). WM, due to its storage and processing components, is viewed as a bimodal flexible system of a limited capacity. Since WM maintains current information and simultaneously supports its execution, as a latent factor underlying intelligence (5), it has been termed as "the central executive" (6) attention-controlling system dependent on consciousness (7). However an awareness-independent model has been also proposed (8,9). General learning (Ln) ability depends on attention and WM interaction (10) as well as perception, the causal and informational ground for the higher cognitive functions (11). Perception guides our thinking about and acting upon the world and serves as an input to cognition, via a short-term memory mediated interactions (12). A possible mechanism linking perception and cognition would be attention (13).

Perception (bottom-up) and cognition (top-down) have been historically viewed as independently operating encapsulating domains. Such embodiment has paved a ground for the view that perceptual experiences can be influenced by cognitive state (for references see 14), consequently elaborated into the brain predictive coding approach currently dominating cognitive neuroscience (15), and positing that attention is a property of brain computation network (16). However this has been challenged by the opposite opinion that "Cognition does not affect perception" (17). Regardless whether or not such a cognitive-sensory dichotomy exists, herein we view perception and cognition as two main information streams the EF exerts its actions upon, possibly through active association.

We have previously described the function of two vertebrate-specific brain-expressed presynaptic gene paralogs, *NTNG1* and *NTNG2*, complementary affecting verbal comprehension and WM in human subjects, which underwent an accelerated evolution in primates and extinct hominins (1). This pair of genes is also implicated in the phenomena of antagonistic pleiotropy, a trade-off between the evolution-driven cognitive function elaboration and an array of concomitant neuropathologies, rendering the human brain phenotypically fragile (2). *Ntngs* also complementary diversify the mouse behavior (18).

Despite the fact that EF abrogation is a major determinant of problem behavior and disability in neuropsychiatric disorders (19), the genetics underlying EF remains elusive with no causative vector agents (e.g. genes) have yet been reported. Herein we show that *NTNG* paralogs affecting human IQ also affect mouse learning and brain executive functioning.

RESULTS

Randomizing mouse genotypes to search for causal behavioral interactions. We used a novel non-parametric data analysis approach for two distinct behavioral paradigms: 5-choice serial reaction time task (5-CSRTT, 20), and radial arm maze (RAM), measuring selective attention and impulsivity (AI), and spatial working memory (WM), respectively, in *Ntng1*$^{-/-}$ and *Ntng2*$^{-/-}$ mice. We calculated mouse genotype-independent ranking (as for a mixed population), and the rank variance (as a proportion of variance explained, PVE) for each behavioral parameter and for both paradigms. This approach allowed us to avoid common in literature a genotype-attributed single parameter reporting bias (Supplementary Figures 1 (SF1) and 2 (SF2)), and permitted us to compare observed phenotypes between the both paradigms for the genetically independent groups of mice, simultaneously searching for potential interactions among them. We were able to follow the dynamics of behavioral heterogeneity and to deduce a causal inference between the mouse phenotypic and genotypic traits interaction affecting executive function (EF).

Affected AI for both *Ntng* paralogs, and WM for the *Ntng2* gene, modulated by the cognitive demand. Analysis of the 5-CSRTT data (ST1-1) has revealed that *Ntng1*$^{-/-}$ population of mice is characterised by an extreme span of its rank distribution (PVE>90%) occupying not only bottom 4 but also top 4 rank positions and outcompeting their wild type littermates (Fig.1(A-D)-1). *Ntng1* ablation generates mice with both strong proficit and deficit of AI, extending far beyond a single affected parameter estimate (Fig.1C,G), but with the averaged rank per a genotype undistinguishable of that of their wild type littermates, and more than 90% of variance attributable to the *Ntng1*$^{-/-}$ genotype (Fig.1A-1). A higher cognitive demand task phase (HCD) reduces the rank variance down to 76% but at the expense of a lower rank (Fig.1E-1), similarly to *Ntng2*$^{-/-}$ mice (Fig.1E-2). During the low cognitive demand task phase (LCD), contrary to *Ntng1*$^{-/-}$ mice, *Ntng2*$^{-/-}$ subjects' rank is twice lower comparing to their genetically unmodified siblings but the rank variances are the same (Fig.1(A-D)-2), and this is the main difference in the AI phenotype between the *Ntng* paralog knockouts, attributable to the magnitude of the demand.

Robustness of the WM deficit upon *Ntng2* deletion in mice is the most prominently evidenced by the bottom 4 mouse ranks, 13/12 out of 16 are occupied by the knockout mice (Fig.2(A-G)-2) and by low behavioral consistency across the sessions and parameters cross-correlations (Fig.2H-2) during the HCD. At the same time, the absence of *Ntng1* in mice affected only the LCD sessions performance (Fig.2(A-D)-1) but did not render them

105 behaviorally distinguishable from the wild type littermates during the HCD (Fig.2(E-H)-1).

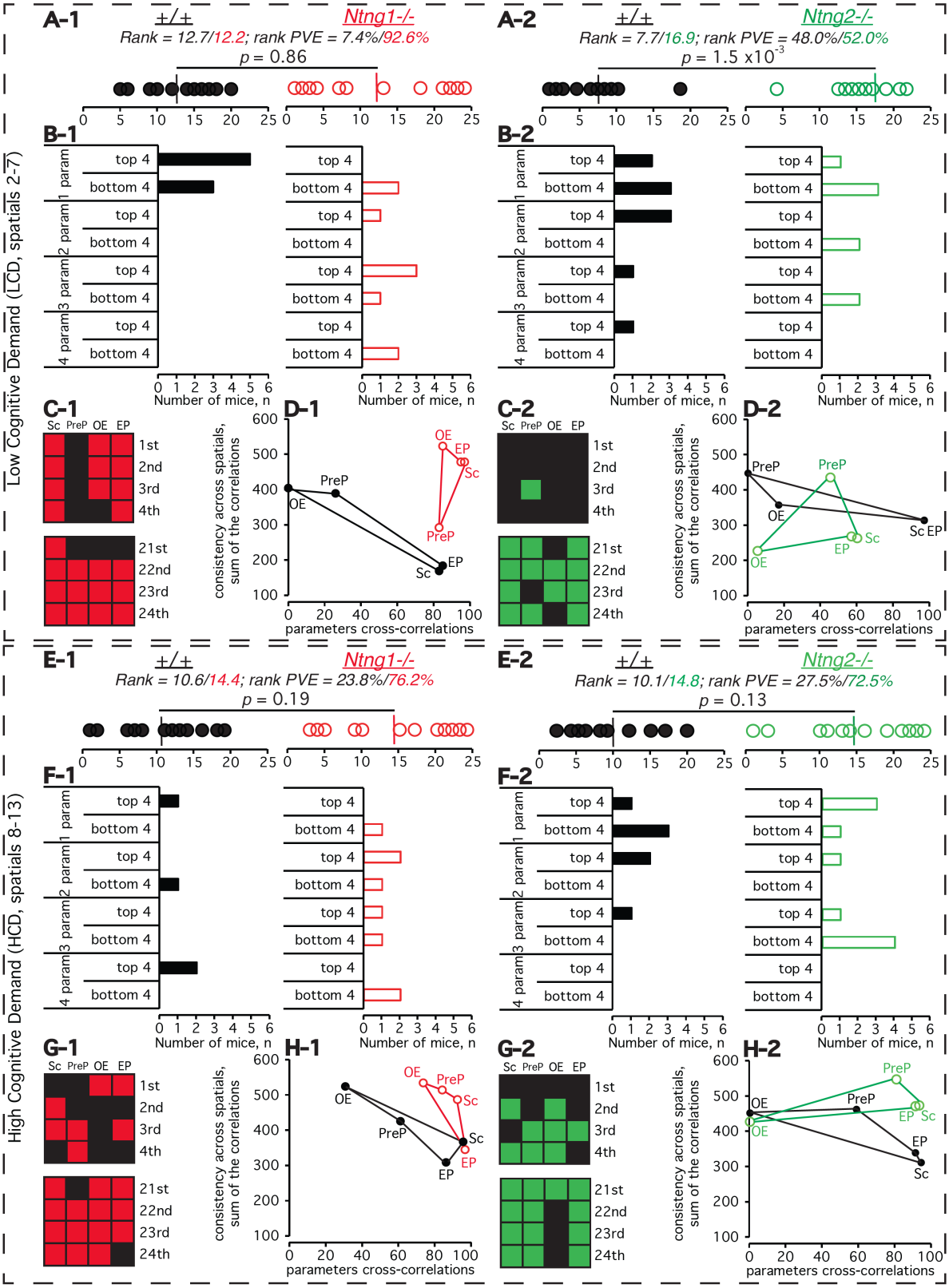

106 Figure 1. 5-choice serial reaction time task (5-CSRTT) for *Ntng1*$^{-/-}$ and *Ntng2*$^{-/-}$ mice. See figure legend overleaf.

107

108 **Proficit and deficit in learning associated with the *Ntng*$^{-/-}$ genotypes.** The intricate

109 segregation of the *Ntng*$^{-/-}$ gene paralogs-associated behavioral phenotypes within the distinct

110 modules of EF (Fig.3) has prompted us to analyse the operant conditioning learning (Ln) by

Figures 1,2. Attention and Impulsivity (AI) and working memory (WM) estimate and the effect of cognitive demand made by the analysis of rank and its variance for *Ntng1*$^{-/-}$ and *Ntng2*$^{-/-}$ mice. **A,E.** Mice ranks and rank PVE (proportion of variance explained) based on four parameter rank measures (SF1,2) as detailed in ST1-1,2-1 (for *Ntng1*$^{-/-}$) and ST1-2,2-2 (for *Ntng2*$^{-/-}$). The rank sorting was done in a genotype-independent manner. Ranking for each out of four parameters was done independently of other parameters with a final re-ranking of the ranks sum to generate the final rank (shown). In case of an equal sum of the ranks, the mice were given identical ranks. PVE was calculated as a square of within genotype rank variance divided on the sum of each genotype variances squares multiplied on 100%. **B,F**. Mice rank distribution across one-to-four parameters as top 4 and bottom 4 performers. **C,G.** Genotype-specific rank placing among the mice. **D,H.** Behavioral consistency of mice across the sessions (*y* axis, sum of r^2 correlations of a single session ranks *vs.* final ranks for each mouse across the sessions) and behavioral parameter cross-correlations (*x* axis, the r^2 correlation of a parameter final ranking *vs.* final ranking for all 4 parameters). The gene ablation-specific phenotype severity can be assessed visually by matching each parameter-corresponding vertexes of the obtained quadruples. *p* value represents a Wilcoxon rank sum test. See SM for further details.

mice, assuming that AI and WM may there interact. And indeed, *Ntng1*$^{-/-}$ mice outperform their control group learning faster during the LCD (Fig.4(A,B)-1, LCD) but are unable to sustainably cope with the growing cognitive demand (Fig.4(A,B)-1, HCD). At the same time, *Ntng2*$^{-/-}$ mice display a prominent deficit of Ln (Fig.4(A,B)-2, LCD), which is becoming stronger with the growing demand to succeed (Fig.4(A,B)-2, HCD). In overall, the pattern of Ln behavior caused by the genetic ablation of both *Ntngs* completely matches that of WM testing on the RAM (Fig.2), summarised in Fig.3**.** The contribution of AI to the Ln deficit is further demonstrated by the rank correlations of Ln *vs.* AI (from Fig.1**)** which is stronger during the HCD for both genetically distinct mouse populations (Fig.4C-1,2).

Complementary expression of *Ntng* paralogs in the brain and their interaction. The robust phenotype of the abrogated EF for both *Ntng* gene paralogs affecting either AI or WM, or both, is supported by the predominant expression of both genes within the heavily loaded with the information processing brain areas, complementary sequestering them within bottom-up (for *Ntng1*) and top-down (for *Ntng2*) neuronal pathways (Fig.5A-C). The presented hierarchy for the *Ntng* paralogs brain distribution is supported by two times lower level of the *Ntng2* expression in *Ntng1*$^{-/-}$ background after the life-long cognitive training in

146 senile mice (Fig.5D-2), with no effect on *Ntng1* expression when *Ntng2* is absent (Fig.5D-1).

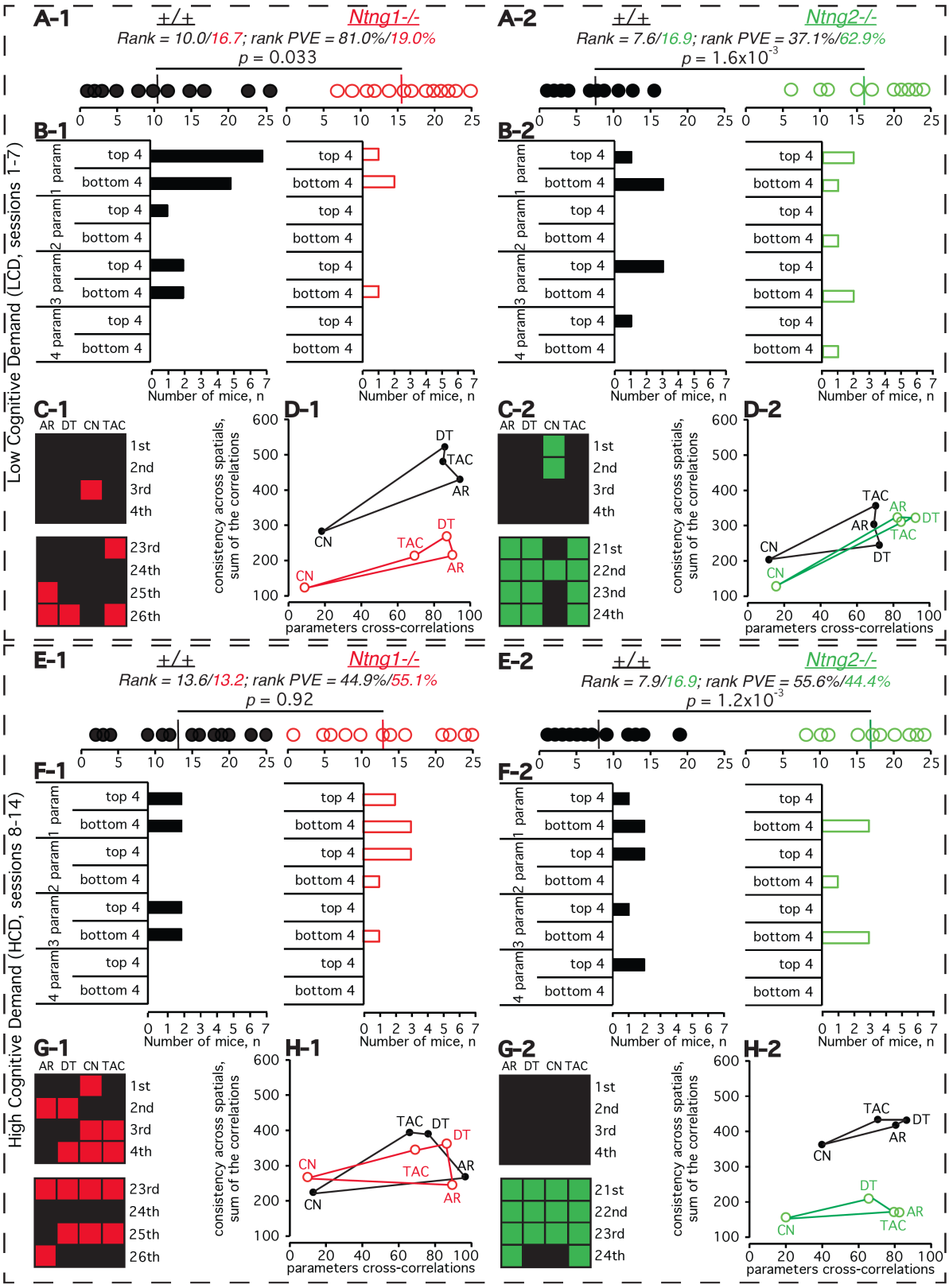

147 Figure 2. Radial arm maze (RAM) for *Ntng1*$^{-/-}$ and *Ntng2*$^{-/-}$ mice. See figure legend overleaf.

148

149 **Robust genotype prediction based on the phenotype input, the rank.** To assess the causal

150 inference of the genes perturbations on behavioral output we have calculated the probability

151 clustering for each genotype based only on the ranking data input, in genotype-blind manner

(Fig.6A). The obtained pattern corroborates the causal relationship between the genotypes and associated with them phenotypes of the affected EF (Fig.3) closely resembling the experimental data (Fig.1.2).

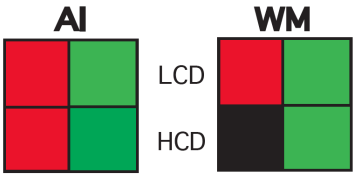

Figure 3. Summary of the EF behavioral phenotypes associated with either *Ntng1*$^{-/-}$ or *Ntng2*$^{-/-}$ gene paralogs ablation.

Mouse behavioral phenotypic proximity assessment. To calculate a phenotypic distance between the genotypes comprising a single mixed population we used the obtained ranks and plotted them against the relted PVE for each behavioral parameter, generating two linear plots (Fig.6B), each representing a single contributing genotype. This let us further to calculate the phenotypic distance (using the classical Euclidean geometry) between the genotypes as the shortest distance between two parallel lines. The obtained geometrical plots are in a full agreement with the experimentally observed behaviors (Figs.1-3) but additionally pinpoin the contribution of each individual parameter sometimes located outside of the main cluster with others, e.g. PreP for the *Ntng1*$^{-/-}$ (Fig.6B-1, AI-LCD), OE for the *Ntng1*$^{-/-}$ (Fig.6B-2, AI-HCD), and CN for the *Ntng2*$^{-/-}$ (Fig.6B-2, WM-LCD). Using the Ln rank and its PVE from Fig.4 as *(x,y)* coordinates we have assessed the phenotypic proximity of the *Ntng1*$^{-/-}$ and *Ntng2*$^{-/-}$ mouse AI and WM phenotypes to the Ln deficit.

Task learning (Ln) as an outcome of AI and MW interactions. With the assumption that shorter distance from the Ln coordinates to the genotype-specific linear plot generates higher likelihood that the given genotype contributes to the Ln associated behavior, we were able to build a relationship graph among the Ln, AI and WM interactions modulated by the cognitive demand (Fig.7A). The dynamics of the *Ntng* gene paralogs hierarchy interaction is presented on Fig.7B, calculated by the reciprocal plug-in of the rank and its PVE for one gene paralog into the linear plot for the other one (ST7).

DISCUSSION

Inferring causal relationship for the *Ntng* paralogs ablation caused perturbations with the EF abrogation phenotypes. The hierarchy of WM and selective attention interplay has been always a point of fierce debate (21). In the present study we look at this interaction through the prism of mouse operant conditioning learning ability, perturbated by either of

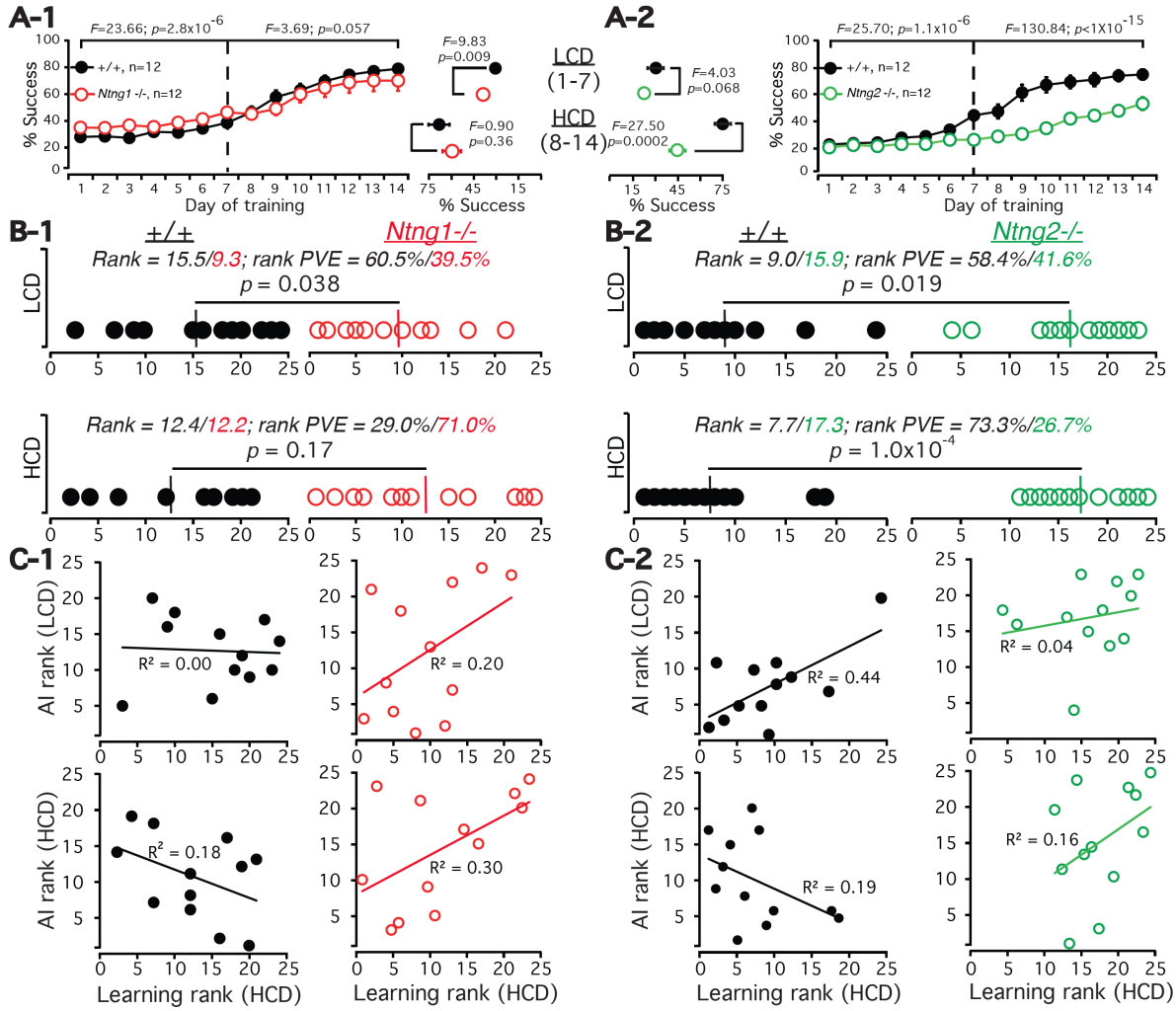

Figure 4. Operant conditioning (5-CSRTT) Learning (Ln) by *Ntng1*$^{-/-}$ and *Ntng2*$^{-/-}$ mice. A. Learning curves for the operant conditioning learning (reward collection) over the training period (spatial 1 of 5-CSRTT) with averaged performance behavior for the days (1-7) and (8-14), middle panel, defined as low cognitive demand (LCD) and high cognitive demand (HCD) sessions, respectively. One and two-way ANOVA was used for the statistics. **B.** Ranks and PVE comparisons over the LCD and HCD. The rank sorting was done in a genotype-independent manner, similar to Fig.1 and Fig.2, but using only one parameter, success (Sc), see ST4-1 and ST4-2. Rank statistics was by Wilcoxon rank sum test. **C.** Learning (Ln) *vs.* attention and impulsivity (AI) rank correlations (from Fig.1A-1,2).

Ntng gene paralogs ablation (Fig.4). Since it is known that averaging animal behavior across individual subjects (SF1-1,1-2) may smear out control variables (22), we used rank instead of classical data mean (Figs.1-3) approach and the rank variance (proportion of variance explained, PVE) per genotype, as a measure of difference (23:p.16), to assess the behavioral variability caused by the genetic variations interacting with the experimental demand. To proof causal inferences between the behavior of *Ntng*$^{-/-}$ mice and the gene ablation, we used mouse rank as a randomized dependent variable of the mixed population noting that any other non-randomized variables would be only correlational (24). That is, we have presented the mouse behavioral rank distribution as a function of genotype, when one of the *Ntng*

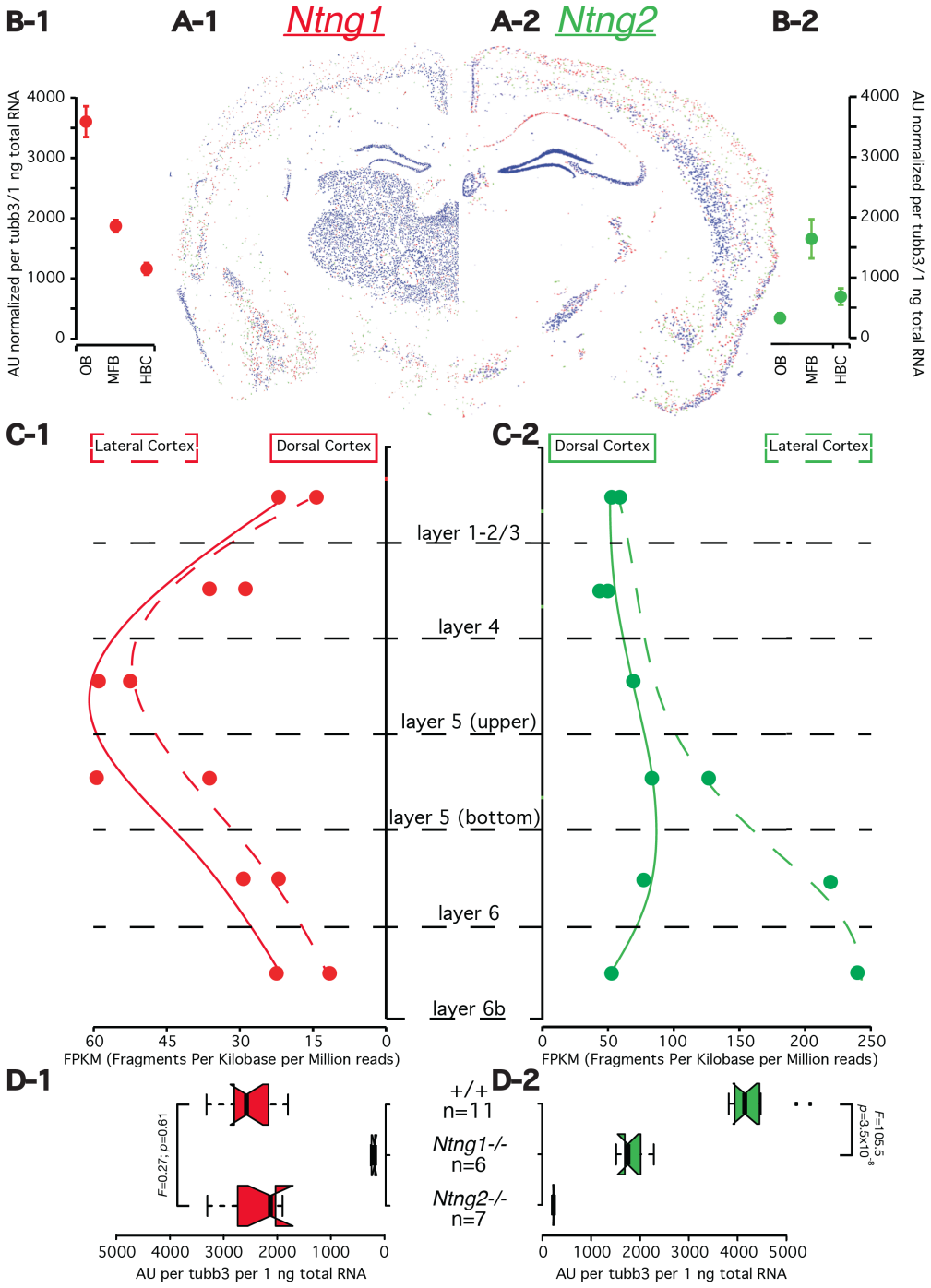

Figure 5. Complementary expression and transcription of *Ntng* paralogs in the mouse brain. (**A**) *In situ* hybridization of *Ntng1* (left) and *Ntng2* (right) in the mouse brain. From Allen Brain Atlas, accession numbers are RP_050607_01_H05 and RP_050810_04_D08, respectively. The expression colors are inverted. (**B**) qRT-PCR of total mRNA for *Ntng* paralogs in rough brain fractions of adult naïve male mice (7-8 months old): OB = olfactory bulb; MFB = mid- and front brain; HBC = hindbrain and cerebellum, n=6 mice (ST5-1). (**C**) Total level of *Ntng* mRNA expression calculated based on RNA-seq of the mouse brain cortical layers reconstructed for *Ntng* paralogs expression from GSE27243 generated by Belgard et al. (51). See Supplementary Methods (SM) for the details of data processing, ST5-2, ST5-2_Cuff and ST5-2_iReck (zipped) for the trascriptome assembly. (**D**) Effect of genetic background on *Ntng* paralogs expression level in MFB as detected by qRT-PCR (ST5-3). Senile (20-21 months old) life-long cognitively trained mice have been used (from Fig.1). One-way ANOVA was used for the statistics.

paralogs has been genetically ablated. At the same time, we have tried to elaborate on the statement that the structure of genotype–phenotype map is the matter and not the variance components of the population itself (25). The open question in such genotype-phenotype

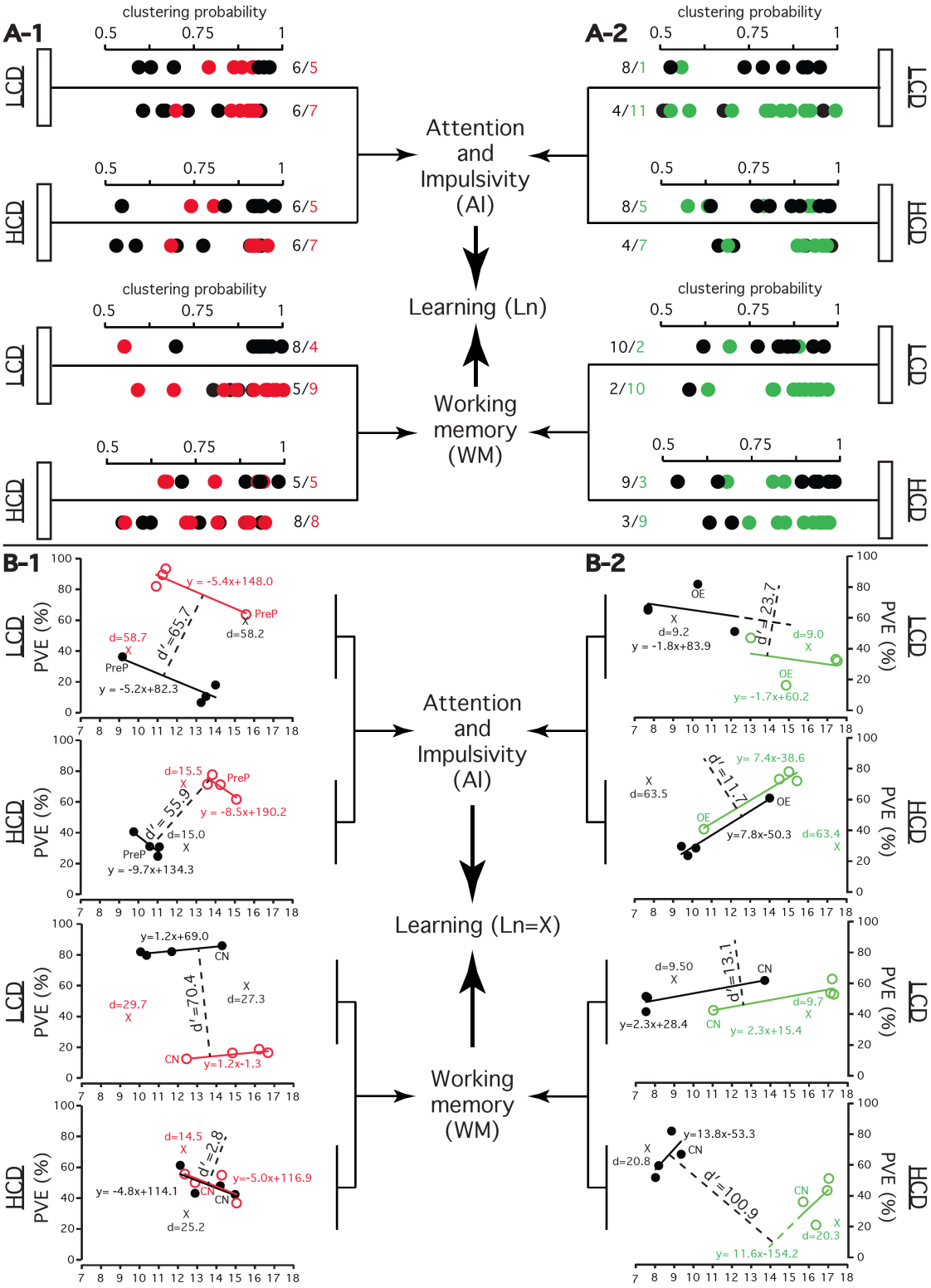

Figure 6. Behavioral phenotypic proximity assessment for the *Ntng1*$^{-/-}$ and *Ntng2*$^{-/-}$ genotypes and their wild type littermates by two approaches: genotype predictions by *C*-means fuzzy clustering (**A**), and by linear regression plot of genotype-specific rank PVE *vs.* rank (**B**). **A.** Casual genotype-phenotype relationship evidence. *C*-means fuzzy clustering (Euclidean *C*-means) was done in a genotype-blind manner as described in SM. See ST6-1 and ST6-2 for the exact values of clustering probabilities. **B.** Descriptive proximity of the operant conditioning learning explained by the AI and WM phenotypes for *Ntng*$^{-/-}$ paralogs mice. Distance between the genotypes (d', dashed line), presented geometrically by the linear equation, was calculated as $d'=|c_2-c_1|$, where $ax+by+c=0$ (Euclidean geometry). Distance from the learning coordinates (Ln) to the genotype-describing line was calculated as $d=|c-(y_{Ln}-ax_{Ln})|$. Rank (*x* coordinates) and PVE values (*y* coordinates) are from Fig. 1A,E (AI); Fig.2A,E (WM); and Fig.4B (Ln), ST7. Data for the *Ntng1*$^{-/-}$/wt population (RAM) are likely to incorporate 7.69% error since they were not normalised to the total number of animals as for the other populations (n=26 *vs.* n=24 mice).

interaction paradigm is to what degree a genetic variability is capacitive enough to explain the phenotypic variance and the strength of such causal interaction. More specifically, how far the behavioral (whole organism) variability (under the pressure of the growing cognitive demand) represents the neuronal (cellular) variability caused by a gene knockout exerted perturbations.

Cognitive phenotypes of the *Ntng*$^{-/-}$ mice. None of the vertebrate brain specific presynaptically expressed *Ntng1*$^{-/-}$ nor *Ntng2*$^{-/-}$ mice exhibit gross anatomical or developmental abnormalities (26) rendering them unique models to study the brain cognitive functions in the absence of any "house-keeping" functional distortions and avoiding gene-manipulations-exerted non-causal confounders. Noteworthy the resemblance of *Ntng1*$^{-/-}$ and *Ntng2*$^{-/-}$ mice behavioral phenotypes with the human schizophrenia subjects behavioral etiology (characterised by the EF control pathologies), both genes have been reportedly associated with (1,2). Two different populations of mice were used for two different behavioral paradigms to avoid the phenomena of learning transfer between the behavioral tests, and, at the same time, to check for the genotype induced phenotypic stability across the different paradigms but sharing the principal underlying component of WM testing. And indeed, slow operant conditioning learning (5-CSRTT) for *Ntng2*$^{-/-}$ mice has been recorded (Fig.4A,B-2) and is explainable by the dysfunction of procedural (working) memory robustly affecting the RAM performance (Fig.2A-H-2).

Behavior consistency assessment using rank. We have also characterised the behavior of mice as a heterogeneously randomized population through the assessment of rank consistency across the sessions and relative to other parameters (Figs.1-2D,H). Parameters cross-correlation coefficients (r^2, *x* axis) indicate a probability value of how much the rank of a mouse for a certain parameter contributes to the global (total) ranking comprised of all four parameters. If a mouse fails to keep its performance consistent either over the multiple sessions or a parameter, its rank is instantly occupied either by the same or by a different genotype littermate, and such event would be dynamically reflected in the r^2. But ranks changes and their permutations may not necessary have any dramatic consequences in the total rank calculations as soon the rank fluctuations are taking place within the same genotype-specific variance boundaries. But they are more reflective of a behavior inconsistency of an individual mouse reflected in the sum of the correlation variances per spatial or session (*y* axis).

WM deficit driven optimal strategy deprivation for the *Ntng2*$^{-/-}$ mice. The global spatial WM deficit for the *Ntng2*$^{-/-}$ mice has been found robustly expressed across the three RAM parameters (Fig.2A-H-2) except for CN (arm choice number during the first 8 arm entries). This parameter represents a strategy development (during LCD) and its optimisation (during HCD) for the maximum reward collection efficiency, akin predictive type behavior of the likelihood of potential success. The fact that the *Ntng2*$^{-/-}$ mice outperform their wt littermates in CN (but during the LCD only, Fig.2C-2) reflects the chosen strategy (or a complete lack of any) of a pure random choice of a baited arm to visit, corroborating the global WM deficit (inability for strategic thinking) for the knockouts (evident from the other parameters) but with an opposite valence.

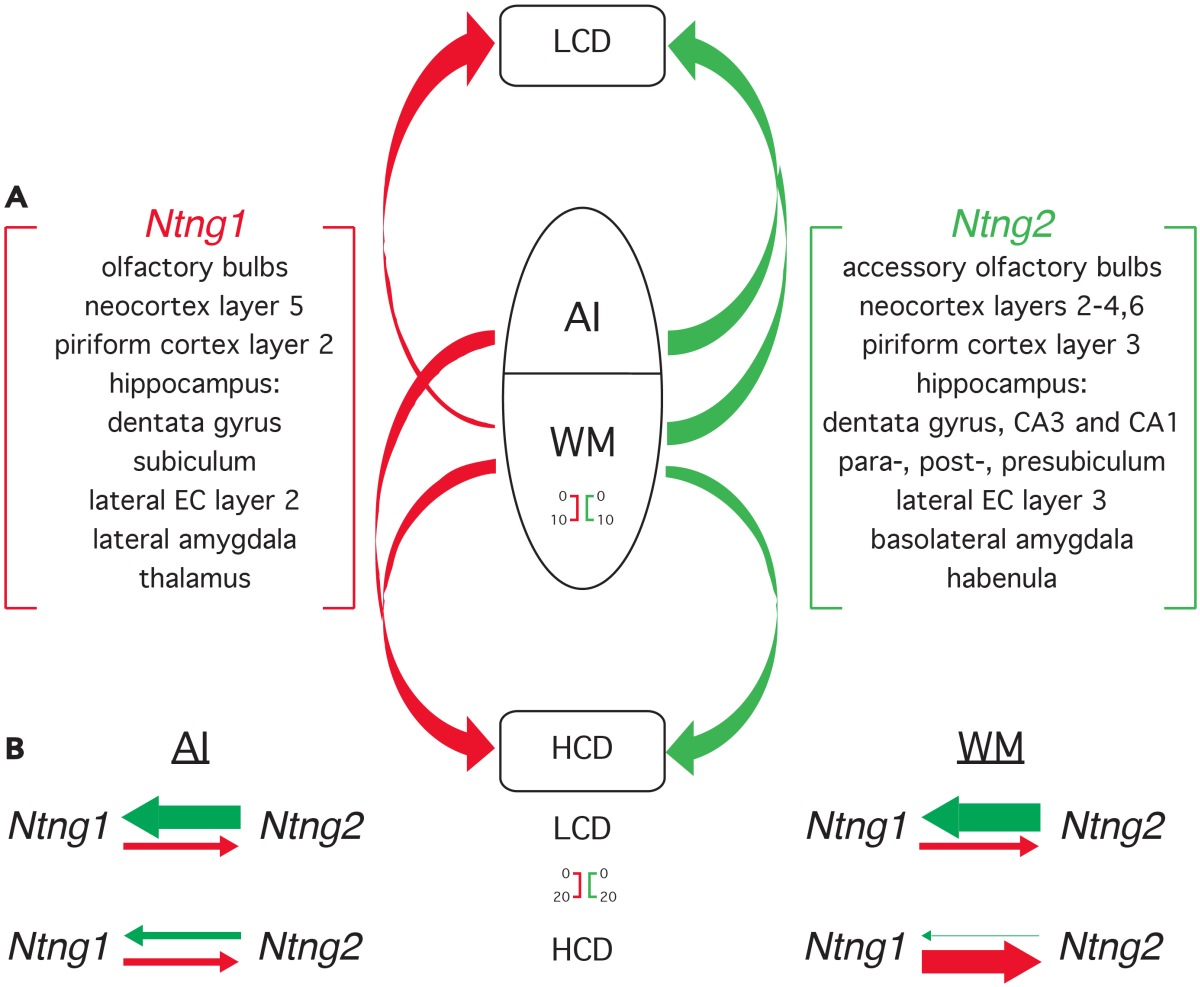

Figure 7. *Ntng* paralogs interaction as a molecular correlate of AI and WM modalities during learning. A. AI and WM interactions modulated by the cognitive demand during the operant conditioning earning (Ln), complementary contributed by the differentially expressed *Ntng* paralogs (see Fig.5 and (52)). B. Dynamicity of *Ntng* paralogs hierarchy interactions under LCD and HCD contributing to AI and WM. Each arrow base width (the scale bar is shown) is expressed in AU and corresponds to (1/d*100) value from Fig.6B (for Ln=X), see ST7. Out of scale arrows (AI-*Ntng1*-LCD and AI-*Ntng2*-HCD) are not shown.

Paralogs brain expression supporting the behavioral phenotypes. The phenotypic

complementarities among the *Ntng1*$^{-/-}$ and *Ntng2*$^{-/-}$ mice, associated either with the abrogated AI or WM, or both (Fig.3), are supported by the complementary brain expression pattern of these gene paralogs (Fig.5A). If *Ntng1* is expressed mostly in the primary somatosensory gating areas (e.g. OB, thalamus and hypothalamus nuclei, midbrain and medulla, Fig.5A,B-1), *Ntng2* dominates within the cortex (with the skewed expression saturation towards the lateral cortex), hippocampus (HPC), amygdala and claustrum, endopiriform and reticular nuclei, Fig5A-2**)**, pointing the gene role of parsing top-down signals. If the sensory perception, as an entry point into the attentional state, is determined by the strength of the subcortical thalamus-PFC (pre-frontal cortex) pathways (27), the reciprocal interactions between mPFC and HPC are pivotal for the WM functioning (28,29), with the HPC known to encode perceptual representations into memories through the correct attentional states (30). Complementing this, thalamocortical projections are vital for mediating sensation, perception, and consciousness (31-33). It is assumed that WM, despite its distributed nature (34), consists of an executive component spread over the frontal lobes and sensory cortices and interacted by the attention (7,35).

Brain lamina-specific enrichment and EF control contribution by the *Ntng* paralogs. The emergence of a six-layered neocortex is a known hallmark of the mammalian brain specialization devoted to the EF control (36,37). Both *Ntng* gene paralogs are extensively expressed and mutually sequestered among the separate layers of the cortex (Fig.5C). *Ntng1* is predominantly located in layers 4/5 (Fig.5C-1), probably supporting the arrival of the bottom-up signals (38), while *Ntng2* is located in the superficial layers 2/3 and deeper layers 5/6 (Fig.5C-2), reported as a source of top-down inputs in attention and WM demanding tasks (39). Besides that, *Ntng2* has been also marked as a gene classifier for the granule neurons enriched in the cortex layer 6 (40). In overall, the complementary patterning of the *Ntng* gene paralogs expression supports the laminar-specific distribution of the attention-directed modalities.

Evidence for the cognitive control taking over the perceptual load. Analysing AI and WM interaction during the task learning (Fig.7A), we have revealed that HCD recruits more *Ntng1* (bottom-up) expressing circuitry comparing to LCD, both by WM and AI, reciprocally replacing the preceding *Ntng2* (top-down) contribution. This potentially points to an augmented peripheral sensory control by upregulating the bottom-up information stream. How to explain such intricacy? Attention exploits a conserved circuitry motif predating the neocortex emergence (41) and WM probably exapts the motor control of forward action

modeling also elaborated since ancient times (42). The archaic origin of both modalities limits the fundamental brain resource and constrains information processing, forcing trade-offs among the objects of targeted attention through the top-down control and, possibly, causing a competition between the sensory inputs (43,44) by driving attention at representations in sensory areas where the latter gains entry into WM (7). A model has been proposed that selective attention control is directly linked to the executive control part of the WM system (45) corroborating the statement that attention and WM should no longer be regarded as two separate concepts, see (46) for references. The top-down control of primary sensory processing by higher cortical areas (through the recurrent inputs) has an essential role in sensory perception, as we have just demonstrated. The pervasive penetration of the cognitive control, supported by *Ntng2,* affects the sensory inputs, provided by the *Ntng1* expression.

An IQ for mice. The EF control variance attributes to the cognitive performance variance and does not exist independently of general intelligence (47) as a critical determinant of human cognition (48). It is no wonder then that, in our hands, the genes affecting WM and attention in mice are the same ones affecting IQ in humans (1) and also associated with a variety of devastating neurological disorders (2) representing a strong case of antagonistic functional pleiotropy. The open challenge is to find out to what degree, using *Ntng* gene paralogs as benchmarks, we would be able to conclusively draw on either domain specific or domain general cognitive abilities of mice, or any other non-human animal subjects behavioral intelligence.

Conclusively, *Ntng1* participates in bottom-up, and *Ntng2* in top-down brain information flows support, representing an integrative complementary agreement between perception and cognition as two interacting functions of the brain.

CONCLUSION

The view of Brain (and Mind) as a modular (domain) system is appealing to evolutionary thinking (49) but is strongly biased towards “the prominence of neural reductionism” (22) dominating the modern neuroscience. There is no strict definition of what a cognitive domain is but it can be viewed as a product of interaction between the top-down and bottom-up underlying neuronal circuits forming bidirectional feedback loops for the executively decisive and sensory information flows controlling its own self. Genes selectively expressed

317 within such circuits via a non-overlapping pattern represent a tantalizing target to study the
318 cognitive domain make-up and its evolution. An ancient *Ntng* gene duplication (>500 million
319 years ago, preceding the Cambrian explosion) and subsequent co-evolution within the
320 vertebrate genomes made *Ntng* gene paralogs to segregate within the top-down and bottom-
321 up evolving information paths, presumably via subfunctionalisation, under the growing
322 ecological demand (first land/water fish met) but different epistatic environment, both gene
323 paralogs are embedded into. Perception and cognition interplay had eventually culminated
324 in a reflectively subjective representation of the external world, also called consciousness,
325 and explicitly controlled by the EF. Unrevealing molecular correlates of the domain-specific
326 cognitive abilities would help us better understand behavior, e.g. to clearly dissect it on
327 actions (as self-generated thoughts) and responses (cue-induced actions), as a decomposable
328 conjunction supporting the robust functioning of the Brain holistic state.
329
330 MATERIALS AND METHODS
331
332 **Animals and behavioral set-ups.** The original behavioral datasets have been partially
333 published by us in (18). All raw data are provided in ST1-ST4 and SF1,2. Knockout animals
334 and the behavioral set-ups are described in (18).
335
336 **Data analysis.** All raw data including their ranks and PVE calculations with all formulas and
337 graphs are presented in ST1-ST4**.** The dynamics of the rank change for a specific parameter
338 over the course of study and its congruence with other parameters is depicted on Figs.1-
339 2D,H. No robustness calculations of the rank distribution pattern resistance to a sequential
340 removal of a single behavioral subject were done; neither estimate for the minimal number of
341 the top/bottom ranks representing the obtained pattern, it was empirically decided to be equal
342 to top and bottom four (Figs.1-2).
343
344 **Definition of LCD and HCD.** During the 5-CSRTT the cognitive demand was incremented
345 by a shorter cue duration and longer inter-trial intervals, as specified in (18). As for the
346 RAM, the second week of testing (sessions 8-14) was done with half-closed/half-opened
347 doors under the gradually building cognitive demand, internally driven by the behavior
348 optimisation strategy for the maximum likelihood of reward collection, top–down executive–
349 attentional pressure to optimise the behavioral performance outcome, contextually similar to
350 the operant conditioning learning (Ln) of spatial 1 of the 5-CSRTT **(**Fig.4**)**.
351

Real-time qPCR (qRT-PCR). Primers specifically targeting beginning of each *Ntng* gene paralogs full-length transcripts were designed using Primer3Plus: http://www.bioinformatics.nl/cgi-bin/primer3plus/primer3plus.cgi. Frozen brains RNA was isolated from the MFB using RNeasy Plus Minikit (Qiagen) and the cDNA was synthesised by the QuantiTect® Reverse Transcription kit (Qiagen) using a mix of the random hexamers and oligodT primers. cDNA synthesised from 1 ng of total RNA was used per a single qRT-PCR reaction. The lack of genomic DNA and the absence of external contamination were confirmed by the RT-minus reactions. Neuronal-specific *tubb3* transcript (β-tubulinIII) was used as an internal normaliser during the qRT-PCR co-amplifications. The C_t values were collected at the threshold value of 0.4 and the arbitrary units (AU) were calculated as:

$$2^{-(Ct\ (amplicon)\ -\ Ct\ (normalizer))} * 10{,}000$$

RNA-seq cortical layers *Ntng* transcriptome reconstruction. See SM for the details.

Fuzzy *C*-Means Clustering. Represents a type of a sequential competitive learning algorithm exhibiting the stochastic approximation problem (50). Was used for the genotype predictions based on the behavioral ranks input under the genotype-blind input conditions. The details are described in the SM.

Statistics. Correlation coefficients (r^2) were obtained with Excel. One and two-way ANOVA was calculated using StatPlus (AnalystSoft Inc.). Wilcoxon rank sum test was done by Matlab (v.7.9.0 2009b) by the function *ranksum.*

SUPPLEMENTARY MATERIALS (SM)

Contain Supplementary Figures (SF1-2), Tables (ST1-7), Methods and References. ST1-ST5 are provided as Excel files.

ACKNOWLEDGEMENTS

This work was in part supported by the "Funding Program for World-Leading Innovative R&D on Science and Technology (FIRST Program)" initiated by the Council for Science and Technology Policy (CSTP), and KAKENHI 15H04290 from the Japan Society for the Promotion of Science (JSPS).

COMPETING INTERESTS

Authors would like to express a lack of any competing interests associated with the work.

387 REFERENCES

388

389 1. Prosselkov P, Hashimoto R, Polygalov D, Ohi K, Zhang Q, McHugh JT, Takeda M, and
390 Itohara, S. (2016) Cognitive endophenotypes of modern and extinct hominins associated
391 with *NTNG* gene paralogs. *Biomedical Genetics and Genomics*, **1**(1): 5–13.
392 http://doi.org/10.15761/BGG.1000103
393 2. Prosselkov P, Polygalov D, Zhang Q, McHugh JT and Itohara S. (2016) Cognitive domains
394 function complementation by *NTNG* gene paralogs. *Biomedical Genetics and Genomics*,
395 **1**(1): 24–33. http://doi.org/10.15761/BGG.1000105
396 3. Mar AC, Horner AE, Nilsson SRO, Alsio J, Kent BA, Kim CH, Holmes A, Saksida LM,
397 Bussey TJ. (2013) The touchscreen operant platform for assessing executive function in
398 rats and mice. *Nature Protocols*, **8**(10): 1985–2005. http://doi.org/10.1038/nprot.2013.123
399 4. Mandelman SD and Grigorenko EI (2011) "Intelligence". In *The Cambridge Handbook of*
400 *Intelligence.* Edited by Sternberg RJ and Kaufmann SB. Cambridge University Press.
401 ISBN: 052173911X.
402 5. Matzel LD and Kolata S. (2010) Selective attention, working memory, and animal
403 intelligence. *Neuroscience and Biobehavioral Reviews*, **34**(1): 23–30.
404 http://doi.org/10.1016/j.neubiorev.2009.07.002
405 6. Baddeley A. (1992) Working Memory. *Science*, **255**(5044): 556–559.
406 http://doi.org/10.1126/science.1736359
407 7. Carruthers P. (2013) Evolution of working memory. *Proceedings of the National Academy*
408 *of Sciences of the United States of America*, **110**(S2): 10371–10378.
409 http://doi.org/10.1073/pnas.1301195110
410 8. Trubutschek D, Marti S, Ojeda A, King J-R, Mi Y, Tsodyks M and Dehaene S. (2016) A
411 theory of working memory without consciousness or sustained activity. *bioRxiv*.
412 http://doi.org/https://doi.org/10.1101/093815
413 9. Soto D and Silvanto J. (2014) Reappraising the relationship between working memory and
414 conscious awareness. *Trends in Cognitive Sciences*, **18**(10): 520–525.
415 http://doi.org/http://dx.doi.org/10.1016/j.tics.2014.06.005
416 10. Leong YC, Radulescu A, Daniel R, DeWoskin V and Niv Y. (2017) Dynamic Interaction
417 between Reinforcement Learning and Attention in Multidimensional Environments.
418 *Neuron*, **93**(2): 451–463. http://doi.org/10.1016/j.neuron.2016.12.040
419 11. Cahen A and Tacca MC. (2013) Linking perception and cognition. *Frontiers in*
420 *Psychology*, **4**: e144. http://doi.org/10.3389/fpsyg.2013.00144

12. Potter MC. (2012) Conceptual Short Term Memory in Perception and Thought. *Frontiers in Psychology*, **3**: e113. http://doi.org/10.3389/fpsyg.2012.00113

13. Brown H, Friston K and Bestmann S. (2011) Active Inference, Attention, and Motor Preparation. *Frontiers in Psychology*, **2**: e218. http://doi.org/10.3389/fpsyg.2011.00218

14. Mroczko-Wąsowicz A. (2016) Editorial: Perception-Cognition Interface and Cross-Modal Experiences: Insights into Unified Consciousness. *Frontiers in Psychology*, **7**: e1593. http://doi.org/10.3389/fpsyg.2016.01593

15. Clark A. (2013) Whatever next? Predictive brains, situated agents, and the future of cognitive science. *Behavioral and Brain Sciences*, **36**(3): 181–204. http://doi.org/10.1017/s0140525x12000477

16. Rosenberg MD, Finn ES, Scheinost D, Constable RT and Chun MM. (2017) Characterizing Attention with Predictive Network Models. *Trends in Cognitive Sciences*, **21**(4): 290–302. http://doi.org/10.1016/j.tics.2017.01.011

17. Firestone C and Scholl CF. (2015) Cognition does not affect perception: Evaluating the evidence for "top-down" effects. *Behavioral and Brain Sciences*, **39**: e229. http://doi.org/https://doi.org/10.1017/S0140525X15000965

18. Zhang Q, Goto H, Akiyoshi-Nishimura S, Prosselkov P, Sano C, Matsukawa H, Yaguchi K, Nakashiba T and Itohara S. (2016) Diversification of behavior and postsynaptic properties by netrin-G presynaptic adhesion family proteins. *Molecular Brain*, **9**(1): e6. http://doi.org/10.1186/s13041-016-0187-5

19. Royall DR, Lauterbach EC, Cummings JL, Reeve A, Rummans TA, Kaufer DI, LaFrance CW, Coffey CE. (2002) Executive Control Function: A Review of Its Promise and Challenges for Clinical Research. *The Journal of Neuropsychiatry and Clinical Neurosciences*, **14**(4): 377–405. http://doi.org/10.1176/jnp.14.4.377

20. Bari A, Dalley JW and Robbins TW (2008) The application of the 5-choice serial reaction time task for the assessment of visual attentional processes and impulse control in rats. *Nature Protocols*, **3**(5), 759–767. http://doi.org/10.1038/nprot.2008.41

21. Abrahamse E, Majerus S, Fias W and Dijck J-P. (2015) Editorial: Turning the Mind's Eye Inward: The Interplay Between Selective Attention and Working Memory. *Frontiers in Human Neuroscience*, **9:** (e616). http://doi.org/10.3389/fnhum.2015.00616

22. Gomez-Marin A and Mainen ZF. (2016) Expanding perspectives on cognition in humans, animals, and machines. *Current Opinion in Neurobiology*, **37**: 85–91. http://doi.org/10.1016/j.conb.2016.01.011

454 23. Laudański LM. (2013) Between Certainty and Uncertainty: Statistics and Probability in
455 Five Units with Notes on Historical Origins and Illustrative Numerical Examples
456 (Intelligent Systems Reference Library) Springer. ISBN-13: 978-3642256967.
457 24. Jazayeri M and Afraz A (2017) Navigating the Neural Space in Search of the Neural Code.
458 *Neuron*, **93**(5), 1003–1014. http://doi.org/10.1016/j.neuron.2017.02.019
459 25. Paixão T and Barton NH. (2016) The effect of gene interactions on the long-term response
460 to selection. *Proceedings of the National Academy of Sciences*, **113**(16): 4422–4427.
461 http://doi.org/10.1073/pnas.1518830113
462 26. Nishimura-Akiyoshi S, Niimi K, Nakashiba T and Itohara S. (2007) Axonal netrin-Gs
463 transneuronally determine lamina-specific subdendritic segments. *Proceedings of the*
464 *National Academy of Sciences of the United States of America*, **104**(37): 14801–14806.
465 http://doi.org/10.1073/pnas.0706919104
466 27. Wimmer RD, Schmitt LI, Davidson TJ, Nakajima M, Deisseroth K, Halassa MM. (2015)
467 Thalamic control of sensory selection in divided attention. *Nature*, **526**(7575): 705–709.
468 http://doi.org/10.1038/nature15398
469 28. Jin J and Maren S. (2015) Prefrontal-Hippocampal Interactions in Memory and Emotion.
470 *Frontiers in Systems Neuroscience*, **9**: e170. http://doi.org/10.3389/fnsys.2015.00170
471 29. Spellman T, Rigotti M, Ahmari SE, Fusi S, Gogos JA, Gordon JA. (2015) Hippocampal–
472 prefrontal input supports spatial encoding in working memory. *Nature*, **522**(7556): 309–
473 314. http://doi.org/10.1038/nature14445
474 30. Aly M and Turk-Browne NB (2016) Attention promotes episodic encoding by stabilizing
475 hippocampal representations. *Proceedings of the National Academy of Sciences of the*
476 *United States of America*, **113**(4): E420-429. http://doi.org/10.1073/pnas.1518931113
477 31. Riga D, Matos MR, Glas A, Smit AB, Spijker S and Oever MCV. (2014) Optogenetic
478 dissection of medial prefrontal cortex circuitry. *Frontiers in Systems Neuroscience*, **8**:
479 E230. http://doi.org/10.3389/fnsys.2014.00230
480 32. John ER. (2002) The neurophysics of consciousness. *Brain Research Reviews*, **39**(1): 1–
481 28. http://dx.doi.org/10.1016/S0165-0173(02)00142-X
482 33. Alitto HJ and Usrey WM. (2003) Corticothalamic feedback and sensory processing.
483 *Current Opinion in Neurobiol.*, **13**(4): 440–445. http://10.1016/S0959-4388(03)00096-5
484 34. Christophel TB, Klink PC, Spitzer B, Roelfsema PR and Haynes J-D. (2017) The
485 Distributed Nature of Working Memory. *Trends in Cognitive Sciences*, **21**(2): 111–124.
486 http://doi.org/10.1016/j.tics.2016.12.007
487 35. Postle BR. (2006) Working memory as an emergent property of the mind and brain.
488 *Neuroscience*, **139**(1): 23–38. http://doi.org/10.1016/j.neuroscience.2005.06.005

36. Smaers JB, Gómez-Robles A, Parks AN and Sherwood CC. (2017) Exceptional Evolutionary Expansion of Prefrontal Cortex in Great Apes and Humans. *Current Biology,* **27**(5): 714-720. http://doi.org/10.1016/j.cub.2017.01.020

37. Hardung S, Epple R, Jäckel Z, Eriksson D, Uran C, Senn V, Gibor L, Yiezhar O, Diester I. (2017) A Functional Gradient in the Rodent Prefrontal Cortex Supports Behavioral Inhibition. *Current Biology,* **27**(4): 549–555. http://doi.org/10.1016/j.cub.2016.12.052

38. Nandy AS, Nassi JJ and Reynolds JH. (2017) Laminar Organization of Attentional Modulation in Macaque Visual Area V4. *Neuron*, **93**(1): 235–246. http://doi.org/10.1016/j.neuron.2016.11.029

39. Kerkoerle T, Self MW and Roelfsema PR. (2017) Layer-specificity in the effects of attention and working memory on activity in primary visual cortex. *Nature Communications*, *8*: e13804. http://doi.org/10.1038/ncomms13804

40. Lake BB, Ai R, Kaeser GE, Salathia NS, Yung YC, Liu R, Wildberg A, Gao D, Fung H-L, Chen S, Vijayaraghavan R, Wong J, Chen A, Sheng X, Kaper F, Shen R, Ronaghi M, Fan J-B, Wang W, Chun J, Zhang, K. (2016) Neuronal subtypes and diversity revealed by single-nucleus RNA sequencing of the human brain. *Science*, **352**(6293): 1586–1590. http://doi.org/10.1126/science.aaf1204

41. Krauzlis RJ, Bollimunta A, Arcizet F, Wang L. (2014) Attention as an effect not a cause. *Trend Cog Sci*, **18**(9): 457–464. http://doi.org/http://dx.doi.org/10.1016/j.tics.2014.05.008

42. Jeannerod M. (2006) *Motor Cognition*. Oxford University Press. ISBN: 0198569653

43. Koch C and Tsuchiya N. (2007) Attention and consciousness: two distinct brain processes. *Trends in Cognitive Sciences*, **11**(1): 16–22. http://doi.org/10.1016/j.tics.2006.10.012

44. Boxtel JJA, Tsuchiya N and Koch C. (2010) Consciousness and attention: on sufficiency and necessity. *Frontiers in Psychology*, **1**: e217. http://doi.org/10.3389/fpsyg.2010.00217

45. Vandierendonck A. (2014) Symbiosis of executive and selective attention in working memory. *Frontiers in Hum Neurosci*, **8**: E588. http://doi.org/10.3389/fnhum.2014.00588

46. Quak M, London RE and Talsma D. (2015) A multisensory perspective of working memory. *Frontiers in Hum Neurosci*, **9**: E197. http://doi.org/10.3389/fnhum.2015.00197

47. Royall DR and Palmer RF. (2014) "Executive functions" cannot be distinguished from general intelligence: two variations on a single theme within a symphony of latent variance. *Frontiers in Behav Neurosci*, **8**: E369. http://doi.org/10.3389/fnbeh.2014.00369

48. Lucenet J and Blaye A. (2014) Age-related changes in the temporal dynamics of executive control: a study in 5- and 6-year-old children. *Frontiers in Psychology*, **5**: E831. http://doi.org/10.3389/fpsyg.2014.00831

523 49. Burkart JM, Schubiger MN and Schaik CP. (2016) The evolution of general intelligence.
524 *Behavioral and Brain Sci*, **Jul 28:** 1–65. http://doi.org/10.1017/S0140525X16000959
525 50. Pal NR, Bezdek JC, and Hathaway RJ. (1996) Sequential Competitive Learning and the
526 Fuzzy *c*-Means Clustering Algorithms. *Neural Networks,* **9**(5): 787–796.
527 51. Belgard TG, Marques AC, Oliver PL, Abaan HO, Sirey TM, Hoerder-Suabedissen A,
528 García-Moreno F, Molnár Z, Margulies EH, Ponting CP. (2011) A Transcriptomic Atlas
529 of Mouse Neocortical Layers. *Neuron*, **71**(4): 605–616.
530 http://doi.org/10.1016/j.neuron.2011.06.039
531 52. Yaguchi K, Nishimura-Akiyoshi S, Kuroki S, Onodera T, Itohara S. (2014) Identification
532 of transcriptional regulatory elements for *Ntng1* and *Ntng2* genes in mice. *Molecuar*
533 *Brain*, **7**(1): 19. http://doi.org/10.1186/1756-6606-7-19